Performance Analysis of Dynamic Spectrum Allocation in Heterogeneous Wireless Networks

Jeounglak Ha, Jin-up Kim, and Sang-Ha Kim

Increasing convergence among heterogeneous radio networks is expected to be a key feature of future ubiquitous services. The convergence of radio networks in combination with dynamic spectrum allocation (DSA) could be a beneficial means to solve the growing demand for radio spectrum. DSA might enhance the spectrum utilization of involved radio networks to comply with user requirements for high-quality multimedia services. This paper proposes a simple spectrum allocation algorithm and presents an analytical model of dynamic spectrum resource allocation between two networks using a 4-D Markov chain. We argue that there may exist a break-even point for choosing whether or not to adopt DSA in a system. We point out certain circumstances where DSA is not a viable alternative. We also discuss the performance of DSA against the degree of resource sharing using the proposed analytical model and simulations. The presented analytical model is not restricted to DSA, and can be applied to a general resource sharing study.

Keywords: Dynamic spectrum allocation (DSA), heterogeneous wireless networks (HWNs), load balancing, resource sharing, radio resource management (RRM).

I. Introduction

Radio communications based on fixed spectrum allocation, which has been well-utilized for decades, faces changes owing to technological convergence and spectrum shortage. Different radio services that were previously disparate are converging and their boundaries blurring. As this convergence may be strengthened in the future, the current static long-term licensing to a single technical standard may hinder fast technical innovation. Moreover, the increased demand for radio spectrum for high-quality mobile multimedia services requires dynamic spatio-temporal spectrum reuse [1]. This dynamic spectrum reuse is being restricted by current regulations.

Spectrum utilization varies temporally and spatially from 15% to 85% [2], while the overall spectrum occupancy measured in Chicago is less than 17.4% [3]. Applying dynamic spectrum allocation (DSA) to the Universal Mobile Telecommunications System (UMTS) and Digital Video Broadcasting-Terrestrial (DVB-T) [1] may increase spectrum efficiency by 29%. Some activities of regulatory agencies and standardization bodies relevant to dynamic spectrum reuse are presented in [4].

DSA aims at exploitation of the underutilized spectrum of other radio systems by incorporating further control to share the spectrum among them. It dynamically allocates a radio spectrum that is not used during certain times or in certain areas. DARPA xG, DIMSUMnet, and IEEE P1900.4 provide framework architectures for DSA. Since DARPA xG [2] is a military project, its opportunistic spectrum use is performed in a distributed manner without any central entity. DIMSUMnet [5] is an architecture for a coordinated DSA by a spectrum broker. IEEE P1900.4 [6] developed a standard in which an operator spectrum manager (OSM) coordinates spectrum

Manuscript received Aug. 31, 2009; revised Mar. 2, 2010; accepted Mar. 11, 2010.

This work was supported by the by the IT R&D program of MKE/KEIT (Ministry of Knowledge Economy/Korea institute of Industrial Technology Evaluation and Planning), Rep. of Korea (2008-F-001-02, Research on environment-adaptive autonomous technologies for mobile wireless access).

Jeounglak Ha (phone: +82 42 860 5403, email: jlha@etri.re.kr) and Jin-up Kim (email: jukim@etri.re.kr) are with the Internet Research Laboratory, ETRI, Daejeon, Rep. of Korea.

Sang-Ha Kim (email: shkim@cnu.ac.kr) is with the Department of Computer Engineering, Chungnam National University, Daejeon, Rep. of Korea.

doi:10.4218/etrij.10.1409.0032

 © 2010 ETRI

usage among networks. The IST-DRiVE project [7] studied the coordinated DSA problem in heterogeneous wireless networks (HWNs), assuming that a common coordinated channel was being used. A framework to achieve dynamic and decentralized spectrum management as well as joint radio resource management (RRM) in HWNs is presented in [8].

The performance gains of DSA using the load history or prediction between UMTS and DVB-T are discussed in [7] and [9]. In [10], the auction based spectrum allocation problem in cellular networks under the coordinated DSA model is addressed. In [11], a DSA system with a packing behavior in open spectrum wireless networks is investigated. Markov chain (MC) based approaches on DSA with primary priority over a secondary user are proposed in [12] and [13]. The primary user preempts the communication channel by cutting off communication of the secondary user.

In this paper, we analyze the performance of DSA using an MC model. A simple DSA algorithm between two radio access technologies (RATs) is proposed, in which DSA decision is based on the performance history and prediction. The two RATs are assumed to have RAT-specific spectrum resources (RSSRs) and have access to a common DSA spectrum resource (CDSR). The RSSR is exclusive to one RAT while the CDSR is shared by both RATs. The previous studies considered all resources to be common for both RATs, but we expect radio communication operators will hold their own radio frequency spectrum for radio networks during the intermediate time before a complete transition to the age of a fully common spectrum. We provide an extensive analysis of the performance results when applying DSA, and discuss its performance gain. Our study finds that DSA may not bring benefits under certain circumstances.

The organization of the paper is as follows. In section II, we describe HWN systems where DSA is applied. Section III discusses a traffic model and provides an analysis of DSA based on a 4-D MC. Numerical results of the analysis are provided in section IV, and our conclusion is given in section V.

II. System Description

1. DSA Architecture

We consider that DSA will be performed in a layered architecture as in Fig. 1. A spectrum broker (SB) [10] manages the overall spectrum usage rights and coordinates access to the spectrum among operators. An OSM [6] manages the spectrum within an operator and coordinates the assignment of the spectrum among the RATs of the operator. A community resource manager (CRM) dynamically assigns spectrum to a local resource manager (LRM) according to the load status of each LRM. The CRM is in charge of load balancing among

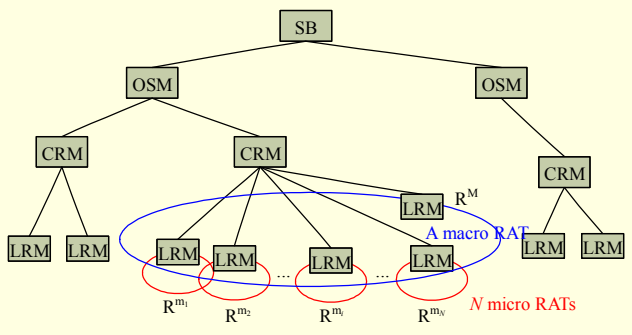

Fig. 1. Dynamic spectrum management architecture for heterogeneous wireless networks.

LRMs within a specified area of a community. A community is a conceptual area where radio resources are managed together. An LRM is similar to a traditional RRM entity with further interaction with a CRM for inter-RAT load balancing. The hierarchical architecture of DSA entities enables various time scale granularities of the DSA cycle and assignment sizes of spectrum among layers.

A. DSA Cycle

A DSA cycle is the time during which DSA is performed periodically. The length can be decided according to the hierarchical location or situation in which it is applied. The timescale of DSA is discussed in [14] and a layered approach of inter- and intra-operator spectrum management is discussed in [8]. DSA among operators, conducted by OSM and SB, may take from minutes to days, while DSA among RATs within an operator, may take milliseconds to seconds. DSA within a RAT, may take microseconds to milliseconds. Online and batched processing models of spectrum demand are mentioned in [15]. The online model processes requests on a call-by-call basis, and the batched model processes requests received during a time window of T units. In [16], an auction within a short interval is shown to respond better to traffic dynamics than that within a longer interval.

This paper defines the DSA cycle as τ, but it is not restricted to a definite timescale. We use the statistical features of traffic during τ in our analytic model and simulation. However, it is natural that a reasonable τ enhances the performance of DSA as well as enables a realistic traffic modeling.

B. Spectrum Allocation Unit

A concept of coordinated access band (CAB), which is a contiguous chunk of spectrum to be reserved by radio regulatory authorities for controlled dynamic access, is introduced in [5]. To the best of our knowledge, however, there is no actual allocation of the CAB by any regulatory authorities

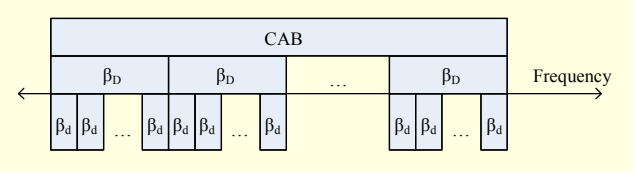

Fig. 2. Spectrum allocation unit.

yet. Following the CAB concept, let Ω denote the amount of spectrum of CAB and β_d denote the basic size of the spectrum to be handled among DSA entities, which may differ according to the center frequency of each CAB; Ω/β_d is then the number of the basic spectrum units of DSA to be allocated.

Since β_d is the basic unit of spectrum management, we introduce an enhanced concept of the spectrum management unit to be dynamically assigned during τ, which is assumed to be a multiple of β_d. Let u be the average arrival rate of users to a DSA entity during τ, and w be the average required bandwidth per user; $\beta_D=u\cdot w$ is then the unit size of the bandwidth to be handled during τ. Figure 2 shows the relations among CAB, β_D, and β_d, where β_D reflects the statistical characteristics of traffic during τ and will be used in the DSA decision. Since there are various types of RATs and their working bandwidths differ, we assume $\beta_D \geq \beta_d$.

2. DSA Decision

For the purpose of a simple presentation, we assume that there are N cells of a RAT that covers the micro range, that one cell of a macro RAT is overlaid within a space under discussion, and that N cells are arranged sequentially and numbered in order as depicted in Fig. 1. They are represented as R^{m_i} and R^M, where m_i is the i-th cell of N cells in the micro RAT, and M is the macro RAT. Given $1/K$ frequency reuse factor, we can define a set of cells, F_k, as

$$F_k = \begin{cases} \left\{ R^{m_i} \,\middle|\, i = k + n\cdot K, n \geq 0, i \leq N \right\}, & \text{if} \quad 1 \leq k \leq K, \\ \{R^M\}, & \text{if} \quad k = K+1. \end{cases} \tag{1}$$

Cells in F_k can reuse the same frequency according to K. Because of the overlaid structure, the spectrum that R^M uses cannot be used by any R^{m_i}. Thus, F_{K+1} serves only R^M.

Variable $\varphi^{F_k}(\tau)$ is the demand for DSA from F_k during τ:

$$\varphi^{F_k}(\tau) = \Big(\Big(\sum_{l=0}^{L} \gamma_{u_l} \rho^{F_k}(\tau - l)\Big) C_u^{F_k} + \Big(\sum_{l=0}^{L} \gamma_{b_l} P_b^{F_k}(\tau - l)\Big) C_b^{F_k} + \Big(\sum_{l=0}^{L} \gamma_{d_l} P_d^{F_k}(\tau - l)\Big) C_d^{F_k} \Big) \cdot |F_k|, \tag{2}$$

where $1 \leq k \leq K+1$. We consider spectrum utilization ρ, new call blocking probability P_b, and handoff call dropping probability P_d together for $\varphi^{F_k}(\tau)$. The considered parameters are defined in vectors for a DSA cycle time. The entire considered time is L units of τ. For each parameter, weighting coefficient γ and cost C are reflected. In order to reflect the number of cells in an F_k group, the cardinality of set F_k, $|F_k|$, is multiplied. It should be noted that parameters at (τ–0) are predicted values. The coefficients for ρ, P_b, and P_d are γ_{u_l}, γ_{b_l}, and γ_{d_l}, respectively, at (τ–l). The averages of ρ, P_b, and P_d of F_k at (τ) are $\rho^{F_k}(\tau)$, $P_b^{F_k}(\tau)$, and $P_d^{F_k}(\tau)$. The costs for ρ, P_b, and P_d of each F_k are $C_u^{F_k}$, $C_b^{F_k}$, and $C_d^{F_k}$.

In order to calculate the required number of spectrum allocation units, $\varphi^{F_k}(\tau)$ is normalized as

$$\varphi^{F_k}(\tau) = \frac{\varphi^{F_k}(\tau)}{\sum_{k=1}^{K+1} \varphi^{F_k}(\tau)} \cdot D, \tag{3}$$

where D is Ω/β_D.

The normalized $\varphi^{F_k}(\tau)$'s are, then, built into a well-ordered set [17] Φ(τ) according to their fractional part,

$$\begin{aligned} &\Phi(\tau) = \left\{ \varphi^{F_k}(\tau) - \left\lfloor \varphi^{F_k}(\tau) \right\rfloor \middle| 1 \leq k \leq K+1 \right\}, \\ &[\Phi(\tau) : F1] \leq [\Phi(\tau) : F2] \quad \text{if} \quad F1 \geq F2, \end{aligned} \tag{4}$$

where [S:F] is the index of F in S, and $\lfloor x \rfloor$ is the largest integer less than or equal to x. It should be noted that Φ(τ) is in decreasing order.

The number of spectrum units to be assigned to F_k during τ is denoted as $\omega^{F_k}(\tau)$ and calculated as

$$\omega^{F_k(\tau)} = \Big(\left\lfloor \varphi^{F_k}(\tau) \right\rfloor + \delta\Big(\Big[\Phi(\tau) : \varphi^{F_k}(\tau) - \left\lfloor \varphi^{F_k}(\tau) \right\rfloor \Big] < D - \sum_{k=1}^{K+1} \left\lfloor \varphi^{F_k}(\tau) \right\rfloor \Big) \Big) \cdot \beta_D / \beta_d, \tag{5}$$

$$\delta(x) = \begin{cases} 1, & \text{if } x \text{ is true} \\ 0, & \text{else} \end{cases}.$$

Since the DSA is performed using the unit of β_d, $\omega^{F_k}(\tau)$ is represented as a number of β_d and is shared among R^{m_i}'s of set F_k.

III. Model Description and Analysis

1. Traffic Model

For simplicity, we assume the statistical characteristics of N cells in the micro RAT are identical, though each has different parameter values. With this, we may consider all m_i's with no discrimination, and represent any m_i as m. Another assumption is that traffic is at a constant bit rate (CBR) and it follows a Markov modulated Poisson process (MMPP). The arrival rates, λ^m and λ^M, follow Poisson processes, and the service time is exponentially distributed with rate μ. Traffic into R^{m_i} is represented by λ^m, and λ^M represents traffic into R^M. Each λ^m and λ^M is an aggregate traffic arrival rate from new calls, λ_n, and from handoff calls from neighboring cells, λ_h. The overall

traffic inflow is modeled as λ and a portion of it is into the micro RAT and the other is into the macro RAT. The portions are defined as $P^m=\lambda^m/\lambda$ and $P^M=\lambda^M/\lambda$. The service time is assumed to be the same for both RATs.

$$\begin{aligned}\lambda^m &= \lambda_n^m + \lambda_h^m \\ \lambda^M &= \lambda_n^M + \lambda_h^M \\ \lambda &= \lambda^m + \lambda^M\end{aligned} \tag{6}$$

Arrival rates λ^m and λ^M and service time μ are modeled in terms of τ duration.

2. Markov Chain

MC models are used in [11]-[13]. An MC model is used for DSA in open spectrum wireless networks in [11]. In [12], forced termination probability, the blocking probability, and system throughput in cognitive radios access in licensed bands are derived using an MC model. A primary-prioritized MC model is proposed in [13] for dynamic spectrum access between the primary and the secondary users. We employ an MC model for probabilistic analysis as [11]-[13] did. In order to build a manageable MC for the CDSR and the RSSRs of two RATs, we have the following settings:

- N=1,
- No handoff call priority,
- $\gamma_{u_0}=0,\ \gamma_{b_0}=\gamma_{d_0}=1$, and perfect knowledge of the traffic in each τ,
- $\gamma_{u_l}=\gamma_{b_l}=\gamma_{d_l}=0$, where $1\le l\le L$,
- $C_u^{F_k}=C_b^{F_k}=C_d^{F_k}=1,\quad \forall k$.

With these settings, we build a 4-D MC of which state (i, di, j, dj) is the resource usage status of the micro and the macro RATs during τ, where i and j are the numbers of the occupied RSSR units of the micro and the macro RATs, respectively. The maximum numbers of the RSSR units for each RAT are defined as I and J. The numbers of the occupied CDSR units of the micro and the macro RATs are di and dj, where $di+dj\le D$. The unit of both RSSR and CDSR is a multiple of β_D.

Because of the complicated nature of 4-D MC model, we first organize the states according to i and j as in Fig. 3. For each i and j, we arrange the states according to di and dj in a triangular shape. The number of states is $(I+1)(J+1)(D+1)(D+2)/2$. The state transition diagram template is depicted in Fig. 4, but the application of each transition arrow depends on the state. State (i, di, j, dj) in Fig. 4 is the case when (i+di) spectrum units are occupied by the micro RAT and (j+dj) are occupied by the macro RAT. The steady state probabilities are $P_{i,di,j,dj}$, and the sum of all $P_{i,di,j,dj}$'s is 1 [18]. Upon arrival of a call to a RAT, the RSSR is primarily used, while the CDSR is used only if the RSSR is not available. Unlike the assumption in [11], we do not pack spectrum resources at their release, but rather the CDSR is open to use by both RATs.

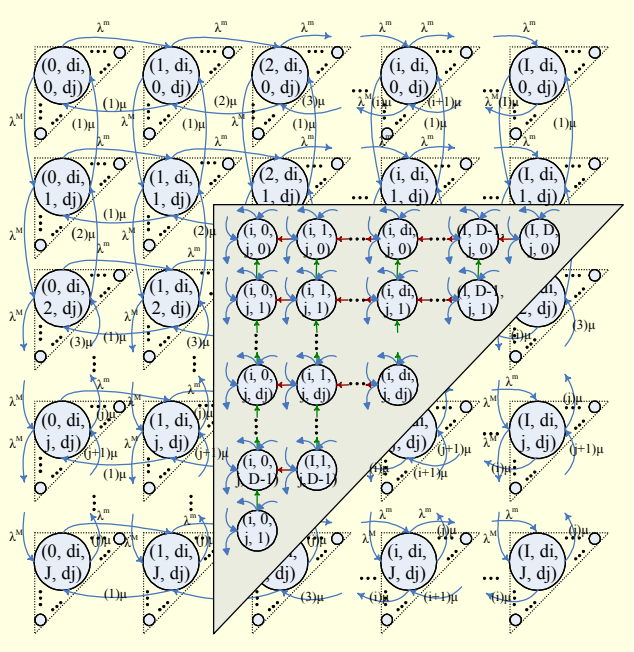

Fig. 3. 4-D state transition diagram framework.

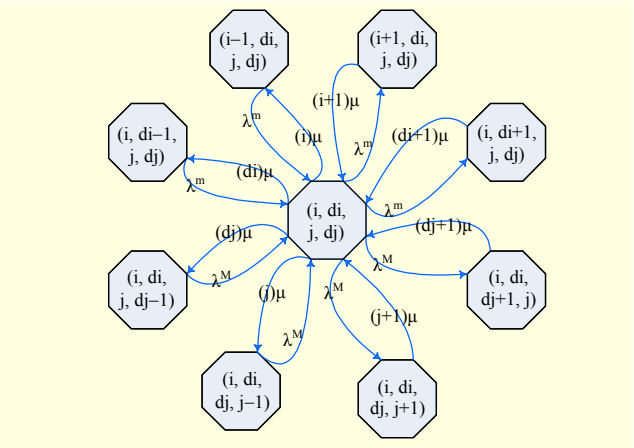

Fig. 4. State transition diagram template.

3. Balance Equations

The number of balance equations (BEQs) in general form is sixty-three. Because of limited space we present the rule for building BEQs rather than BEQs themselves. Combining the BEQ space and the BEQ generating rule together, we may build BEQs.

A. Balance Equation Space

The domain of state (i, di, j, dj) depicted in Fig. 3 is [0,I] × [0,D] × [0,J] × [0,D], where [a,b]={$x\in\mathbb{N}_0$: a≤x≤b, $\mathbb{N}_0$ is a

natural number including 0}. In order to formulate the general form BEQs, the categories of i and j domains are defined as sets $\mathbb{I}$ and $\mathbb{J}$:

$$\begin{aligned}\mathbb{I} &= \{'(i=0)',\ '(0<i<I)',\ '(i=I)'\},\\ \mathbb{J} &= \{'(j=0)',\ '(0<j<J)',\ '(j=J)'\}.\end{aligned} \tag{7}$$

The categories of di and dj domains are defined as set $\mathbb{D}$:

$$\mathbb{D} = \begin{Bmatrix} '(di=0,dj=0)',\ '(0<di<D,dj=0)', \\ '(di=D,dj=0)',\ '(di=0,0<dj<D)', \\ '(di=0,dj=D)',\ '(0<di,dj<D)', \\ '(0<\overline{di,dj})' \end{Bmatrix}, \tag{8}$$

where di,dj is for $di>0, dj>0$, and $di+dj<D$,
$\overline{di,dj}$ is for $di>0, dj>0$, and $di+dj=D$.

Unlike $\mathbb{I}$ and $\mathbb{J}$, which organize states in a square, $\mathbb{D}$ defines di and dj together to form a triangular shape of each (i,j) as in Fig. 3.

The states in Fig. 3 can be represented using the domain sets $\mathbb{I}$, $\mathbb{J}$, and $\mathbb{D}$ as

$$\mathbb{S} = \left\{ P_{i,di,j,dj} \,\middle|\, (i)\in\mathbb{I}, (j)\in\mathbb{J}, (di,dj)\in\mathbb{D} \right\}. \tag{9}$$

The BEQs of $(I+1)(J+1)(D+1)(D+2)/2$ states are reduced to sixty-three BEQs in general form as defined in $\mathbb{S}$.

B. Balance Equation Generating Rule

The universal form of a BEQ is given by

$$\begin{aligned} &P_{i,di,j,dj}(\lambda^{\mathrm{m}}) + P_{i,di,j,dj}(\lambda^{\mathrm{M}}) + P_{i,di,j,dj}((i)\mu) \\ &\quad + P_{i,di,j,dj}((di)\mu) + P_{i,di,j,dj}((j)\mu) + P_{i,di,j,dj}((dj)\mu) \\ &= P_{i+1,di,j,dj}((i+1)\mu) + P_{i,di+1,j,dj}((di+1)\mu) \\ &\quad + P_{i,di,j,dj+1}((dj+1)\mu) + P_{i,di,j+1,dj}((j+1)\mu) \\ &\quad + P_{i-1,di,j,dj}(\lambda^{\mathrm{m}}) + P_{i,di-1,j,dj}(\lambda^{\mathrm{m}}) + P_{i,di,j,dj-1}(\lambda^{\mathrm{M}}) \\ &\quad + P_{i,di,j-1,dj}(\lambda^{\mathrm{M}}). \end{aligned} \tag{10}$$

This reflects all state transitions shown in Fig. 4. It should be noted that λ^{m} from $P_{i,di,j,dj}$ is applied only once, and so is λ^{M}. An arrival of traffic occupies spectrum resources of either RSSR or CDSR.

Since the universal form of BEQ incorporates all possible transitions, irrelevant transitions are to be eliminated according to i, di, j, and dj. The elimination rules are given from (10a) to (10g).

$$\begin{aligned} P_{i,di,j,dj}((i)\mu) &= 0 \quad \text{if} \quad i=0, \\ P_{i,di,j,dj}((j)\mu) &= 0 \quad \text{if} \quad j=0. \end{aligned} \tag{10a}$$

$$\begin{aligned} P_{i,di,j,dj}((di)\mu) &= 0 \quad \text{if} \quad di=0, \\ P_{i,di,j,dj}((dj)\mu) &= 0 \quad \text{if} \quad dj=0. \end{aligned} \tag{10b}$$

Equations (10a) and (10b) show that there is no release of resources if there is no occupied traffic on the RSSR or the CDSR.

$$\begin{aligned} P_{i,di,j,dj}(\lambda^{\mathrm{m}}) &= 0 \quad \text{if} \quad i=I \wedge (di+dj)=D, \\ P_{i,di,j,dj}(\lambda^{\mathrm{M}}) &= 0 \quad \text{if} \quad j=J \wedge (di+dj)=D. \end{aligned} \tag{10c}$$

Equation (10c) shows that if all spectrum resources are used up, no new traffic can be accepted. Traffic to each RAT is blocked if both RSSR and CDSR are completely occupied.

$$\begin{aligned} P_{i+1,di,j,dj}((i+1)\mu) &= 0 \quad \text{if} \quad i=I, \\ P_{i,di,j+1,dj}((j+1)\mu) &= 0 \quad \text{if} \quad j=J. \end{aligned} \tag{10d}$$

Equation (10d) shows that the $(i+1)$th state or $(j+1)$th state does not exist if the RSSR is already used up.

$$\begin{aligned} P_{i,di+1,j,dj}((di+1)\mu) &= 0 \quad \text{if} \quad (di+dj)=D, \\ P_{i,di,j,dj+1}((dj+1)\mu) &= 0 \quad \text{if} \quad (di+dj)=D. \end{aligned} \tag{10e}$$

Equation (10e) shows that the $(di+1)$th state or $(dj+1)$th state does not exist if the CDSR is already used up.

$$\begin{aligned} P_{i-1,di,j,dj}(\lambda^{\mathrm{m}}) &= 0 \quad \text{if} \quad i=0, \\ P_{i,di,j-1,dj}(\lambda^{\mathrm{M}}) &= 0 \quad \text{if} \quad j=0. \end{aligned} \tag{10f}$$

Equation (10f) shows that the $(i-1)$th state or $(j-1)$th state does not exist if $i=0$ or $j=0$.

$$\begin{aligned} P_{i,di-1,j,dj}(\lambda^{\mathrm{m}}) &= 0 \quad \text{if} \quad di=0 \vee i<I, \\ P_{i,di,j,dj-1}(\lambda^{\mathrm{M}}) &= 0 \quad \text{if} \quad dj=0 \vee j<J. \end{aligned} \tag{10g}$$

Equation (10g) shows that the $(di-1)$th state or $(dj-1)$th state does not exist if $di=0$ or $dj=0$. It also shows that traffic is accepted primarily by the RSSR, not by the CDSR if the RSSR remains.

4. Performance Metrics

The performance metrics considered are traffic blocking probability (TBP), dynamic spectrum access probability (DSP), and average throughput (ATP). The TBP is a combined measure to include both traditional new call blocking probability and handoff call dropping probability. Since our model does not consider handoff call's priority over a new call, the two probabilities are merged into and represented by the TBP. However, the call blocking probability and the call dropping probability of the micro RAT are $\lambda_{\mathrm{n}}^{\mathrm{m}}/\lambda^{\mathrm{m}}$ and $\lambda_{\mathrm{h}}^{\mathrm{m}}/\lambda^{\mathrm{m}}$ portion of the TBP, respectively, and $\lambda_{\mathrm{n}}^{\mathrm{M}}/\lambda^{\mathrm{M}}$ and $\lambda_{\mathrm{h}}^{\mathrm{M}}/\lambda^{\mathrm{M}}$ portions are applied to those of the macro RAT from (6). The DSP is the likelihood of using the CDSR when the RSSR is not available.

The state sets where the traffic is blocked and where DSA is

required to accept the traffic are defined as

$$P^{\mathrm{mD}} = \{P_{I,di,j,dj} \mid 0 \le j \le J, 1 \le di, 1 \le dj, di + dj = D\},$$
$$P^{\mathrm{MD}} = \{P_{i,di,J,dj} \mid 0 \le i \le I, 1 \le di, 1 \le dj, di + dj = D\}, \quad (11)$$

and

$$P^{\mathrm{mT}} = \{P_{I,di,j,dj} \mid 0 \le j \le J, 1 \le di, 1 \le dj, di + dj < D\},$$
$$P^{\mathrm{MT}} = \{P_{i,di,J,dj} \mid 0 \le i \le I, 1 \le di, 1 \le dj, di + dj < D\}, \quad (12)$$

respectively. The P^{mD} and P^{MD} states are the rightmost states arranged diagonally in the triangles of each j and i, in Fig. 3, where I or J resources are used up. State sets P^{mT} and P^{MT} are the other states left in the same triangles with the exception of P^{mD} and P^{MD}.

The TBP and the DSP of the micro and the macro RATs, and their average are defined as

$$P^{\mathrm{m}}_{\mathrm{b_{DSA}}} = \sum_{P_s \in P^{\mathrm{mD}}} P_s,$$
$$P^{\mathrm{M}}_{\mathrm{b_{DSA}}} = \sum_{P_s \in P^{\mathrm{MD}}} P_s, \quad (13)$$
$$P^{\mathrm{avg}}_{\mathrm{b_{DSA}}} = P^{\mathrm{m}} \cdot P^{\mathrm{m}}_{\mathrm{b_{DSA}}} + P^{\mathrm{M}} \cdot P^{\mathrm{M}}_{\mathrm{b_{DSA}}},$$

and

$$P^{\mathrm{m}}_{\mathrm{DSA}} = \sum_{P_s \in P^{\mathrm{mT}}} P_s,$$
$$P^{\mathrm{M}}_{\mathrm{DSA}} = \sum_{P_s \in P^{\mathrm{MT}}} P_s, \quad (14)$$
$$P^{\mathrm{avg}}_{\mathrm{DSA}} = P^{\mathrm{m}} \cdot P^{\mathrm{m}}_{\mathrm{DSA}} + P^{\mathrm{M}} \cdot P^{\mathrm{m}}_{\mathrm{DSA}},$$

respectively. Because the overall traffic inflow is divided into both RATs, the TBP and the DSP are multiplied by P^{m} and P^{M} to get average probability of both RATs.

The ATP of the micro and the macro RATs, and their average are defined as

$$T^{\mathrm{m}}_{\mathrm{DSA}} = \Sigma_{\forall(i,di,j,dj)} P_{i,di,j,dj} \cdot (i + di) \cdot \theta^{\mathrm{m}} \cdot \beta_D,$$
$$T^{\mathrm{M}}_{\mathrm{DSA}} = \Sigma_{\forall(i,di,j,dj)} P_{i,di,j,dj} \cdot (j + dj) \cdot \theta^{\mathrm{M}} \cdot \beta_D, \quad (15)$$
$$T^{\mathrm{avg}}_{\mathrm{DSA}} = P^{\mathrm{m}} \cdot T^{\mathrm{m}}_{\mathrm{DSA}} + P^{\mathrm{M}} \cdot T^{\mathrm{M}}_{\mathrm{DSA}},$$

where θ^{m} and θ^{M} are the average spectral efficiencies [19] of each RAT.

In order to compare the performance gain of the proposed DSA, M/M/C/C [18] is used for no-resource sharing (NRS), assuming C is the same with D spectrum units of β_D, the spectral efficiencies θ^{m} and θ^{M} are 1, and the arrival rates of the two RATs and service time follow λ^{m}, λ^{M}, and μ of the proposed model. The average TBP of the two RATs is then represented as

$$P^{\mathrm{avg}}_{\mathrm{b_{NRS}}} = P^{\mathrm{m}} \cdot P^{\mathrm{m}}_{\mathrm{b_{NRS},I}} + P^{\mathrm{M}} \cdot P^{\mathrm{M}}_{\mathrm{b_{NRS},J}},$$

where $P^{\mathrm{m}}_{\mathrm{b_{NRS},s}} = \dfrac{\left(\frac{\lambda^{\mathrm{m}}}{\mu}\right)^s / s!}{\Sigma_{k=0}^{s}\left(\frac{\lambda^{\mathrm{m}}}{\mu}\right)^k / k!}$ and $P^{\mathrm{M}}_{\mathrm{b_{NRS},s}} = \dfrac{\left(\frac{\lambda^{\mathrm{M}}}{\mu}\right)^s / s!}{\Sigma_{k=0}^{s}\left(\frac{\lambda^{\mathrm{M}}}{\mu}\right)^k / k!}$.

The ATP of NRS is defined as

$$T^{\mathrm{m}}_{\mathrm{NRS}} = \Sigma_{s=0}^{I} P^{\mathrm{m}}_{s} \cdot s,$$
$$T^{\mathrm{M}}_{\mathrm{NRS}} = \Sigma_{s=0}^{J} P^{\mathrm{M}}_{s} \cdot s, \quad (16)$$
$$T^{\mathrm{avg}}_{\mathrm{NRS}} = P^{\mathrm{m}} \cdot T^{\mathrm{m}}_{\mathrm{NRS}} P^{\mathrm{M}} \cdot T^{\mathrm{M}}_{\mathrm{NRS}}.$$

Lastly, the performance gain of DSA is defined as

$$\mathbb{G}_{\mathrm{DSA}} = (T^{\mathrm{avg}}_{\mathrm{DSA}} - T^{\mathrm{avg}}_{\mathrm{NRS}}) \cdot \tau \cdot \zeta_b - \lambda \cdot P^{\mathrm{avg}}_{\mathrm{DSA}} \cdot \zeta_{\mathrm{DSA}}, \quad (17)$$

where $\mathbb{G}_{\mathrm{DSA}}$ is the average operating gain, against NRS, of the two RATs applying DSA during τ, ζ_b is the cost of a bit, and ζ_{DSA} is the cost of a single DSA action. In (17), we assume ζ_b is same in both the micro and the macro RATs.

The performance gain of DSA depends on various parameters, and it may be negative at times. An investigation is required into whether or not applying DSA is beneficial for target systems.

IV. Numerical Results

The total number of spectrum units is 15, where I=9 and J=6 for NRS case, and I=7, J=4, and D=4 for DSA. The traffic portion of each RAT is set as P^{m}=0.6 and P^{M}=0.4. The nominal utilization, $\rho_N=\lambda/(C\cdot\mu)$, is set from 0.2 to 0.6, where C is (I+J+D=15). The actual overall system load, ρ, is $C^*\rho_N$, which is 3 to 9 Erlang. The load on the micro RAT, RAT1, is $\rho^{m}=P^{m}*\rho$ and the load on the macro RAT, RAT2, is $\rho^{M}=P^{M}*\rho$. Since the DSA cycle τ is variable, our analysis and simulation results are based on the nominal load during τ, which is ρ_N.

Figure 5 shows the TBP, ATP, and DSP. The performance of DSA is compared to NRS in Figs. 5(a) and 5(b). The solid line is the theoretical result, and the dotted line is from simulation. The simulation is executed 10000τ, and the results match well with analytical results as we averaged out results from extensive rounds of simulations. The average TBPs of both RATs are reduced from about 6.7% to about 3.4% at ρ_N=0.6. The ATP of both RATs is increased by about 10%. Figure 5 (b) assumes both θ^{m} and θ^{M} are 1bit/second/Hz, and β_D is 1MHz. Figure 5(c) shows that the action of DSA grows as the utilization increases. It demonstrates that the performance improvements in Figs. 5(a) and 5(b) are earned by the DSA activities which bring about further space to serve more traffic. The performance differences of RAT1 and RAT2 come from the load differences. Since RAT2 has a much smaller number of the RSSR units considering its traffic load, its request for DSA is higher than that of RAT1. Thus, the performance gain of RAT2 is also bigger than that of RAT1. RAT2 has four RSSR units and receives 40% of the overall traffic, while RAT1 has seven units and receives 60% of the overall traffic.

Figure 6 shows the performance gain of DSA, $\mathbb{G}_{\mathrm{DSA}}$, in (17).

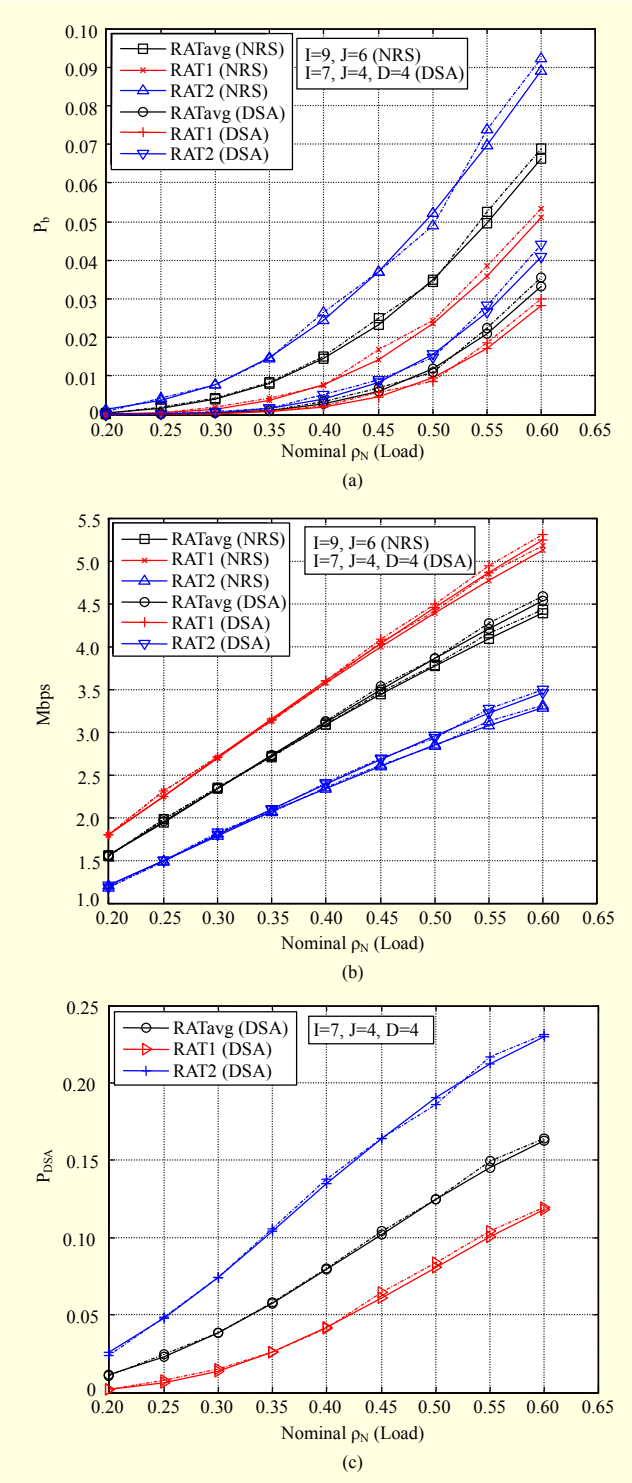

Fig. 5. DSA performance: (a) TBP comparison to NRS, (b) ATP comparison to NRS, and (c) DSA probability.

This figure demonstrates the validity of the throughput gain in Fig. 5(b). Considering the cost of DSA in relation to the cost of a bit and load on the system, there may be a break-even point where applying DSA is beneficial. As the cost of a single DSA

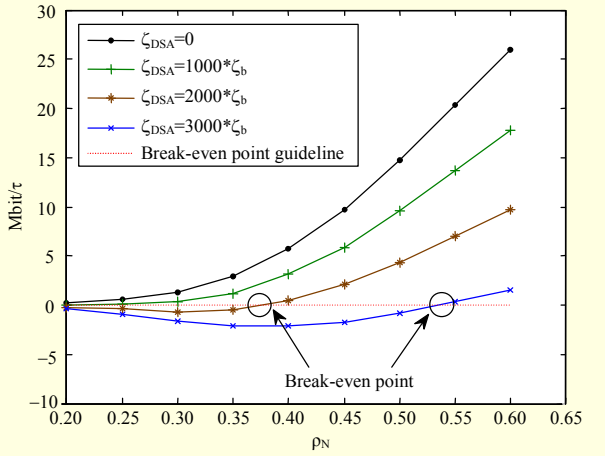

Fig. 6. DSA performance gain.

action grows, the break-even point of nominal utilization moves to a position with high traffic load. In other words, there is a specific point of traffic load on the system where DSA is useful and the point is relative to the cost of DSA. The break-even point is subject to the entire architecture of DSA and system environments.

Figures 7 to 9 compare the performance against the amount of shared spectrum units by changing the RSSR into the CDSR. For all three figures, (a), (b), and (c) stand for different proportions of P^m and P^M. The figures show how DSA works on different loads on each system. The overall spectrum unit is 15, and ρ_N is fixed at 0.6. The X and Y axes show the amount of the RSSR units of the macro RAT and the micro RAT, respectively. The rest of their RSSR units are shared as the CDSR. For all three figures, the Z axis of Fig. 7 is the average TBP, of Fig. 8 is the ATP, and of Fig. 9 is the DSP. The X and Y axes of Figs. 8(a) and 8(b), and Figs. 9(a) through 9(c), are interchanged to show the change in performance more clearly.

In the cases of P^m=0.7 and P^M=0.3, the load on the micro RAT is much higher than that on the macro RAT. Considering that their RSSRs change from 9 to 1 and from 6 to 1, the load on the micro RAT is more intensive. In the cases of P^m=0.5 and P^M=0.5, the load on the macro RAT is higher than that on the micro RAT. In the case of P^m=0.6 and P^M=0.4, the load difference on both RATs is marginal.

In Fig. 7(a), the change of the TBP is greatly dependent on the RSSR of the macro RAT rather than that of the micro RAT. The amount of spectrum units that the micro RAT shares does not have a great impact on the performance, but the amount of shared spectrum units from the macro RAT is very significant. This is because the excessive traffic of the micro RAT may use the shared spectrum units from the macro RAT. In Fig. 7(b), the situation is reversed as the load on the micro RAT is much less

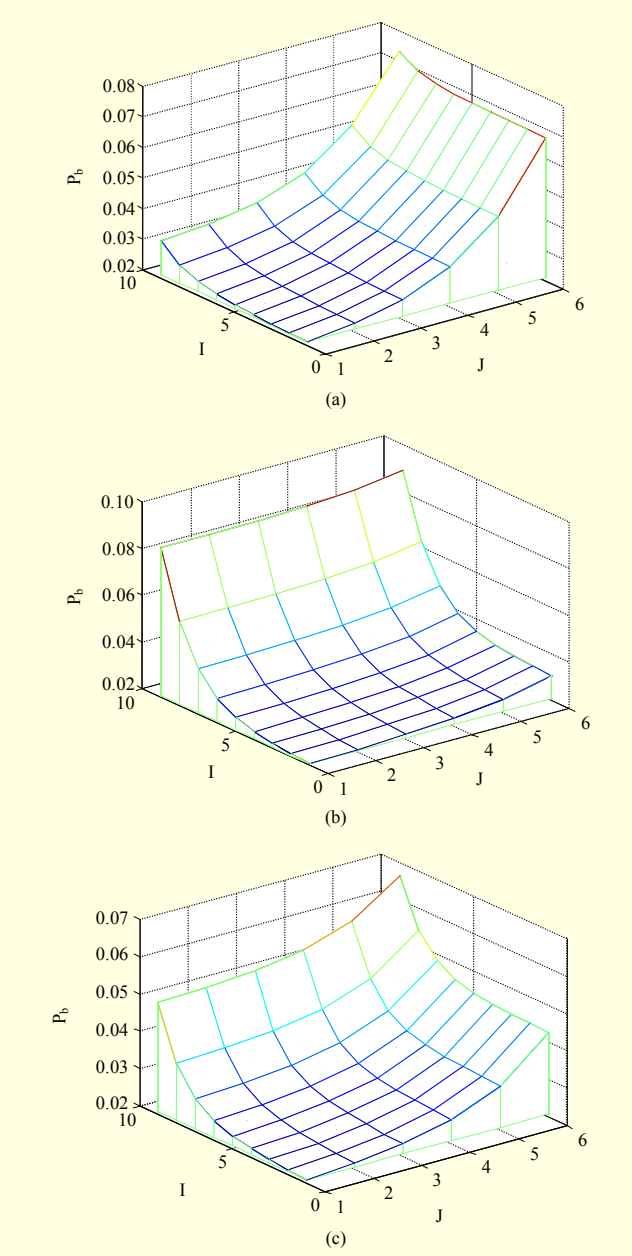

Fig. 7. TBP against degree of the CDSR: (a) P^m=0.7, P^M=0.3; (b) P^m=0.5, P^M=0.5; and (c) P^m=0.6, P^M=0.4.

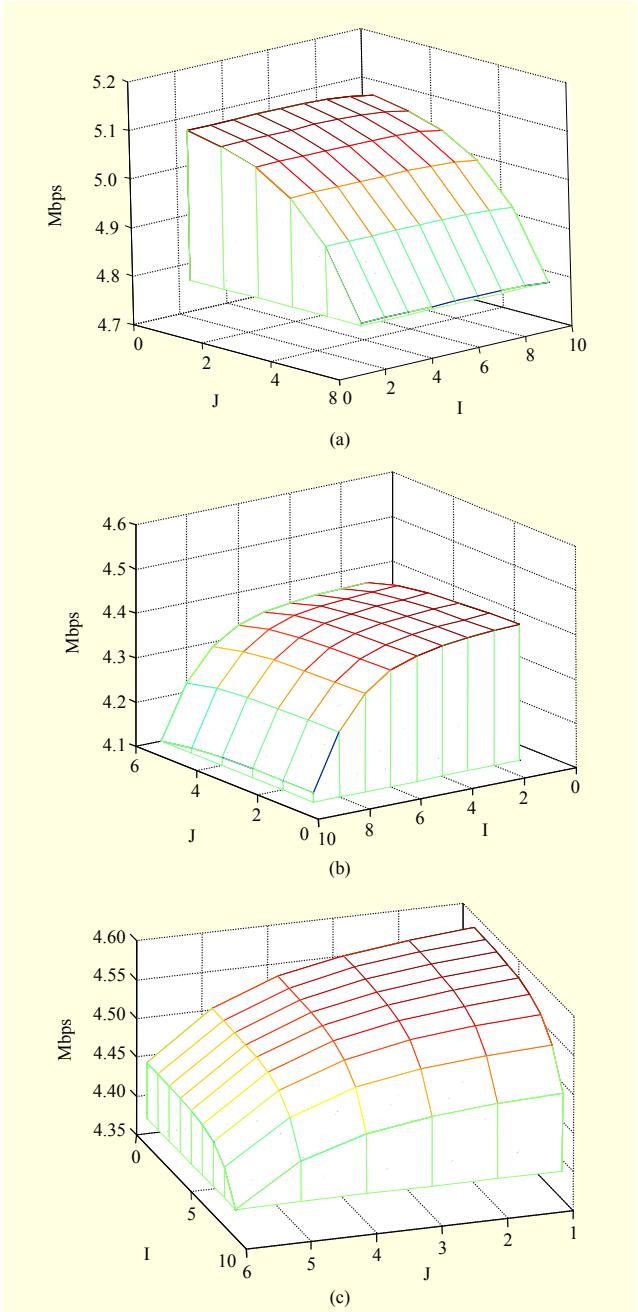

Fig. 8. ATP against degree of the CDSR: (a) P^m=0.7, P^M=0.3; (b) P^m=0.5, P^M=0.5; and (c) P^m=0.6, P^M=0.4.

than that of the macro RAT. Figure 7(c) shows that the performance fairly depends on the change of both RATs sharing the RSSRs as the CDSR. This is because, considering their resources, the load levels of both RATs are similar.

In Fig. 8(a), the ATP greatly depends on the change in the macro RAT RSSR as in Fig. 7(a). The ATP is increased as the macro RAT shares its RSSR as the CDSR. In Fig. 8(b), the ATP greatly depends on the change of the micro RAT RSSR. The ATP in Fig. 8(c) slightly depends on the change of the RSSRs of both RATs. In an overall sense, the effect of sharing the RSSR as the CDSR on the throughput is similar to that on the TBP.

In Figs. 9(a) through 9(c), the probability of DSA action grows linearly as the amount of the CDSR changed from the RSSRs of both RATs is increased. The change of the RSSR of one RAT does not drastically change the probability of DSA action. This trend is different from Figs. 7 and 8. The impact of the load difference on each RAT is not as significant as that in the TBP or the ATP. The overall load on both RATs is more important to DSA usage as shown in Fig. 5(c). This is

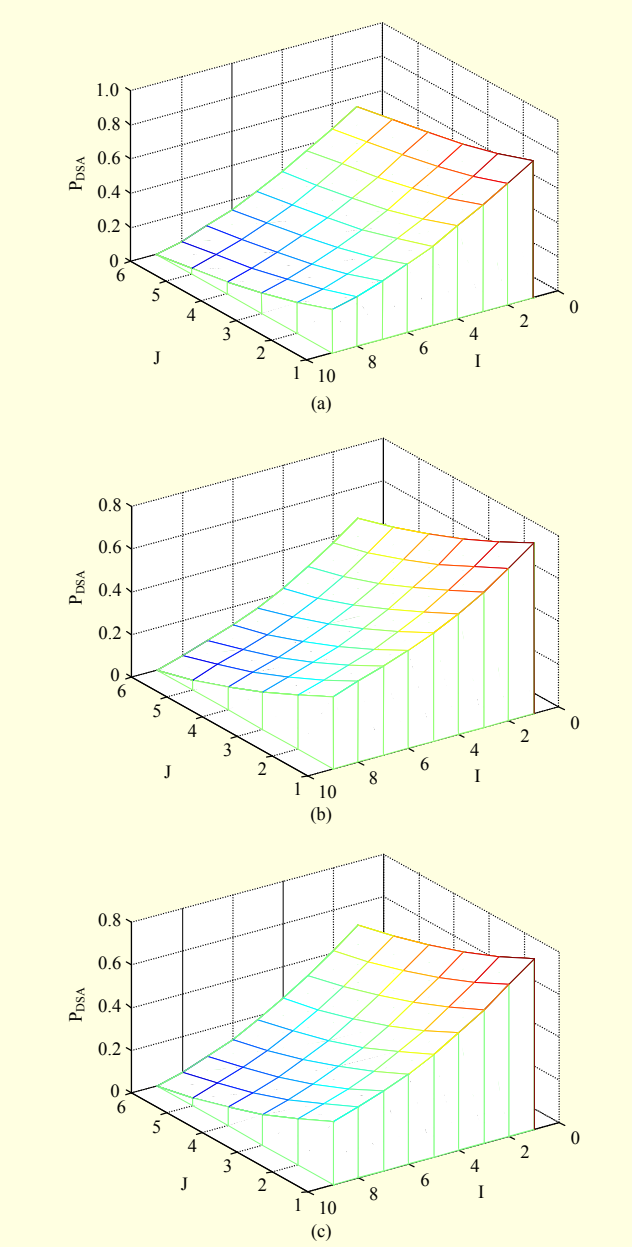

Fig. 9. DSA probability against degree of the CDSR: (a) P^m=0.7, P^M=0.3; (b) P^m=0.5, P^M=0.5; and (c) P^m=0.6, P^M=0.4

because the probability of DSA action is increased regardless of how busy the RAT that shares its RSSR as the CDSR is. The drastic gain of the TBP in Fig. 7 and the ATP in Fig. 8 comes from making use of the CDSR changed from the RSSR of a less busy RAT for a busier one. However, the less busy RAT still has to use DSA even if it shares its RSSR as the CDSR for the other RAT.

V. Conclusion

Dynamic spectrum management is being focused upon in order to save radio resources among converged radio networks and services. Previous works analyzed the performances of DSA that use common spectrum resources in a coordinated or opportunistic manner. We notice that during the transition period to the full-DSA era, determination of whether or not to apply DSA on the existing spectrum allocation is required. This paper provides an analytical model of DSA with the CDSR as well as the RSSR. A 4-D MC is employed to model the RSSRs and the shared CDSR between two RATs. The analytical model is based on a system with a simple spectrum allocation decision algorithm. We discussed the performance of DSA in terms of the TBP, ATP, and DSP. We pointed out there may exist a break-even point of applying DSA in a system. Even though DSA seems to be a promising technique to resolve spectrum shortage, our research result claims that there is a break-even point in employing DSA. The break-even point depends on the system load and the relative cost of DSA to the cost of a bit of the system. The proposed analytical model is a general one so as to be employable in other resource sharing systems. The performance enhancement of DSA was analyzed in terms of the amount of shared spectrum resources.

We are going to study different levels of DSA activity and cost models of DSA with joint RRM among RATs, by which we will further find more concrete resource utilization models under HWN environments.

References

[1] P. Leaves et al., "Dynamic Spectrum Allocation in Composite Reconfigurable Wireless Networks," *IEEE Commun. Magazine*, vol. 42, no. 5, May 2004, pp. 72-81.

[2] I.F. Akyildiz et al., "NeXt Generation/Dynamic Spectrum Access/Cognitive Radio Wireless Networks: A Survey," *Computer Networks,* vol. 50, no. 13, 2006, pp. 2127-2159.

[3] M.A. McHenry et al., "Spectrum Occupancy Measurements, Chicago, Illinois," *Shared Spectrum Company Project Report*, Nov. 2005.

[4] J.A. Hoffmeyer, "Regulatory and Standardization Aspects of DSA Technologies-Global Requirements and Perspective," *New Frontiers in Dynamic Spectrum Access Networks (DySPAN)*, 2005, pp. 700-705.

[5] M. Buddhikot et al., "DIMSUMnet: New Directions in Wireless Networking Using Coordinated Dynamic Spectrum," *Int. Symp. World of Wireless Mobile and Multimedia Networks (WoWMoM)*, 2005, pp. 78-85.

[6] S. Buljore et al., "Architecture and Enablers for Optimized Radio Resource Usage in Heterogeneous Wireless Access Networks: The IEEE 1900.4 Working Group," *IEEE Commun. Mag.*, vol. 47, no. 1, Jan. 2009, pp. 122-129.

[7] P. Leaves, J. Huschke, and R. Tafazolli, "A Summary of Dynamic

Spectrum Allocation Results from DRiVE," *IST Mobile and Wireless Telecommun.*, 2002, pp. 245-250.

[8] O. Sallent et al., "Decentralized Spectrum and Radio Resource Management Enabled by an On-demand Cognitive Pilot Channel," *Annals of Telecommun.,* vol. 63, no. 5-6, Apr. 2007, pp. 281-294.

[9] P. Leaves et al., "Dynamic Spectrum Allocation in a Multi-radio Environment: Concept and Algorithm," *3G Mobile Commun. Technologies*, Mar. 2001, pp. 53-57.

[10] A.P. Subramanian et al., "Near-Optimal Dynamic Spectrum Allocation in Cellular Networks," *New Frontiers in Dynamic Spectrum Access Networks (DySPAN)*, Oct. 2008.

[11] Y. Xing et al., "Dynamic Spectrum Access in Open Spectrum Wireless Networks," *IEEE J. Sel. Areas in Commun.*, vol. 24, no. 3, Mar. 2006, pp. 626-637.

[12] X. Zhu, L. Shen, and T.S. Yum, "Analysis of Cognitive Radio Spectrum Access with Optimal Channel Reservation," *IEEE Commun. Lett.*, vol. 11, no. 4, Apr. 2007, pp. 304-306.

[13] B. Wang et al., "Primary-Prioritized Markov Approach for Dynamic Spectrum Allocation," *IEEE Trans. Wireless Commun.*, vol. 8, no. 4, Apr. 2009, pp. 1854-1865.

[14] K. Moessner et al., "Dynamic Radio Resource Allocation Strategies and Time Scales," *Software Defined Radio Technical Conf.*, Nov. 2005.

[15] M. Buddhikot and K. Ryan, "Spectrum Management in Coordinated Dynamic Spectrum Access Based Cellular Networks," *Int. Symp. New Directions in Dynamic Spectrum Access Networks (DySPAN)*, Nov. 2005, pp. 299-307.

[16] X. Zhou et al., "Traffic-Driven Dynamic Spectrum Auctions," *Sensor, Mesh and Ad Hoc Communications and Networks Workshops (SENCON)*, 2008.

[17] P. Komjath and V. Totik, *Problems and Theorems in Classical Set Theory*, New York: Springer, 2006, pp. 23-36.

[18] L. Kleinrock, *Queueing Systems Volume 1: Theory*, Wiley-Interscience, 1975.

[19] W.G. Chung et al., "Calculation of Spectral Efficiency for Estimating Spectrum Requirements of IMT-Advanced in Korean Mobile Communication Environments," *ETRI J.*, vol. 29, no. 2, Apr. 2007, pp.153-161.

Jeounglak Ha received the BEng and MEng degrees in computer engineering from Kyung Hee University, Seoul, Korea, in 1992 and 1994, respectively. He has been with ETRI, Daejeon, Korea, since 1994. He has researched in the field of the mobile communication networks. His recent research interests include dynamic spectrum management and cognitive radio technologies.

Jin-up Kim received the BS degree from Korea University, Seoul, Korea, in 1985, and MS and PhD degrees from Korea Advanced Institute of Science and Technology, Seoul, Korea, in 1987 and 1996, respectively. He has been with ETRI since 1987. Also, he has been a professor at the University of Science and Technology in the field of wireless communications since 2005. He has researched in the field of the wireless communication systems. His recent research interests include digital RF, software defined radio, and cognitive radio technologies.

Sang-Ha Kim received the BS degree in chemistry from Seoul National University, Seoul, Korea, in 1980. He received the MS and PhD degrees in quantum scattering and computer science from the University of Houston, Houston, TX, in 1984 and 1989, respectively. From 1990 to 1991, he was with the Supercomputing Center, SERI, Korean Institute of Science and Technology (KIST) as a senior researcher. He joined Chungnam National University, Daejeon, Korea, as a professor in 1992. His current research interests include wireless networks, QoS, optical networks, and network analysis. Dr. Kim is a member of ACM, IEEE Communications Society, and IEEE Computer Society.